Structural Safety Assessment for Three-dimensional Distribution Vehicle-Bridge System of Automated Container Terminal under Environmental Loads

[1]Lu Kai-liang

[*1]*Logistics Engineering College, Shanghai Maritime University, China*
lkl1984@163.com

Abstract

An efficient, smart, energy-saving automated container terminal (ACT) scheme is introduced in this paper, in which one three-dimensional container distribution system is proposed between crane yard and storage yard. In this scheme, container vehicle-low bridge coupled vibration greatly affects the ACT's structural safety and handling efficiency. Firstly, the coupled vibration time-domain responses, inspired by self-excitation including track irregularity and hunting movement as well as environmental (wind and seismic) load, were obtained by using free-interface component mode synthesis (CMS) method. The relationship of response and vehicle speed, wind velocity and ground motion intensity was studied as well. Accordingly, the structural safety, running safety and stationarity were assessed by indicators such as deflection-span ratio, vibration acceleration, wheel-rail relative displacement, etc. The container vehicle speed limits of the low bridge rigid supported or lead rubber bearing (LRB) supported under seismic and operational wind load were compared. The results of model test and prototype simulation prove with each other, which validates LRB's effects on vibration isolation and absorption, thus can increase ground motion intensity and vehicle speed thresholds to structural safety.

Keywords: *Automatic Container Terminal, Structural Safety Assessment, Free-interface Component Mode Synthesis, Vehicle-bridge Coupled Vibration, Model Test, Lead Rubber Bearing*

1. Introduction

Through investigation into automation and informatization of the container terminals all over the world, the development of automatic container terminals can be positioned into three stages. The first generation as the representative of Rotterdam port European Combined Terminals (ECT) wharf I and II, uses the semi-automatic quayside container crane, Automatic Guide Vehicle (AGV) with driving speed of 3m/s and automatic yard gantry crane; The second generation as the representative of Hamburger Hafen (CTA) wharf, uses double-container-double-trolley semi-automatic container crane (made by Shanghai Zhenhua Heavy Industry (Group) Co., Ltd., "ZPMC" for short), twin-traction AGV with speed of 5.8m/s and double-track rail-mounted gantry cranes which can stack container and fetch container at the same time; The third generation as the representative of EUROMAX wharf is in the construction designed by ECT wharf. Its equipment configuration is similar to the previous two, but the speed of AGV has increased to 20m/s, the management software system has become more advanced as well.

Container transportation between crane yard and storage yard is implemented usually by AGVs, which have many drawbacks, such as, high capitalized cost, low efficiency, and

serious interference among AGVs. Virtual Reality simulation for automatic container terminal (ACT) scheme illustrated in Figure 1 presents one three-dimensional container distribution system between crane yard and storage yard. Compared to existing ACTs, this scheme has many advantages: (1) Three-dimensional transportation replaces the ground planer way, which solves the AGVs' interference problem. (2) The container vehicles no longer rely on GPS navigation and positioning system, but adopt a more convenient and more accurate orbital positioning. (3) The container vehicle and truss bridge distribution system is less expensive than the AGV system. Last but not the least, green power drive of the entire system is utilized and thus operating cost is reduced.

In this scheme, the low bridge suffers from moving load, container weight and vehicle self-weight. Wheel and rail interaction under self-excitations as track irregularity and hunting movement, external excitations including wind and seismic load, induces lateral and vertical coupled vibration which in turn affects the operating safety and stationarity of vehicle and bridge system. Studies on the coupled vibration of the vehicle and truss bridge system are the necessity of structure safety performance and handling efficiency. The results can be the basis of structure health monitoring, life prediction, optimal design and related industry standard's development.

Vehicle and bridge coupled vibration research has been largely carried out in the area of rail transportation [1-5]. Many factors affect the vibration of vehicle-bridge (VB) system, including self-excitation (track irregularity and hunting movement, *etc*.) and external excitation (wind and seismic load, *etc*.). At present, multi-rigid body-spring-damper discrete model is adopted as the vehicle model while FEM model as bridge model. Then the system equation is formed through wheel-rail interaction. The equation is solved in the time domain due to time-varying. Two main external excitations of VB system are wind and seismic loads. Many researchers have studied the VB system coupled vibration, such as long-span cable stayed bridges or suspension bridges, under disturbing wind [1, 3, 4] or seismic circumstances [5]. Both wind or earthquake effect on vertical and lateral vibration was presented and safe speed limit was gained.

Wheel-rail interaction is usually treated in the following three ways: (1) Both measured track irregularity and hunting movement are assumed to be the wheel-rail interaction [1-2]. (2) Measured or artificial profile of bogie frame hunting movement is considered as the system input [3]. (3) The creep force and kinematical relation of the wheel-rail model can be calculated iteratively by rolling contact theory, such as Hertz theory [4]. Among the three ways, only the last one is able to determine the contact point and contact force of wheel and rail precisely. However, this procedure is very complicated. If the aim is not the wheel- rail kinematical relation but the coupled vibration of VB system, the first two methods are reasonably effective.

The free-interface component mode synthesis (CMS) is very popular because of high efficiency and convenient combination with the experimental modal technique. Interface compatibility conditions can be considered approximately as wheel-rail interaction. Vehicle and bridge is combined to one entire system for coupled vibration analysis [1, 2, 6, 7].

Generally speaking, safety assessment for bridge structure mainly includes: (1) Evaluation of bearing capacity: bridge structure in the aspects of strength, stiffness, stability, whether or not to meet the existing transport load requirements. (2) Durability assessment: fatigue damage and remaining life so far. (3) Applicability evaluation: travelling safety, running stationarity, and passenger comfort, *etc.* [8, 9]. At present, a variety of bridge evaluation technology, calculation model of bridge safety and bridge evaluation expert system had evolved on the basis of fuzzy mathematics and artificial neural network theory. Introducing the method of mathematical analysis, system engineering and other related fields is also

expanded the connotation and extension of the assessment of bridges. Bridge safety assessment methods mainly include: (1) Survey method based on the appearance; (2) Expertise evaluation method; (3) Analytic hierarchy process; (4) Fuzzy comprehensive evaluation method; (5) Methods based on the theory of structural reliability; (6) Method based on damage mechanics and fatigue fracture; (7) Methods based on design specification, *etc.* [10, 11].

In this paper, by using free-interface CMS method, the coupled vibration time-domain responses of the three-dimensional distribution VB system in the ACT under environmental loads were obtained, and the structural safety, running safety and stability were evaluated.

2. Structural Coupled Vibration Analysis of the Three-Dimensional Distribution VB System in ACT

2.1. System Components

As shown in Figure 1, this structural system includes container crane, container vehicle-truss bridge system, ground railway, and ground rotary container vehicle, *etc*. Container distribution procedure is described as follows and vice versa: firstly, crane 1 lifts one container from one vessel to one container transport vehicle 3 seated on the low bridge 2. Secondly, the transport vehicle 3 runs and reaches certain position in high speed and then the container is lifted down to one ground rotary container vehicle 4 by one lifting vehicle 5. Thirdly, the ground vehicle 4 with one container drives to the storage yard 7 on the track 6.

The braces and truss beams of the bridge are linked in full rigid (weld and bolt connection) or full flexible (LRB connected) way. Overall size of the low bridge is shown in Figure 2.

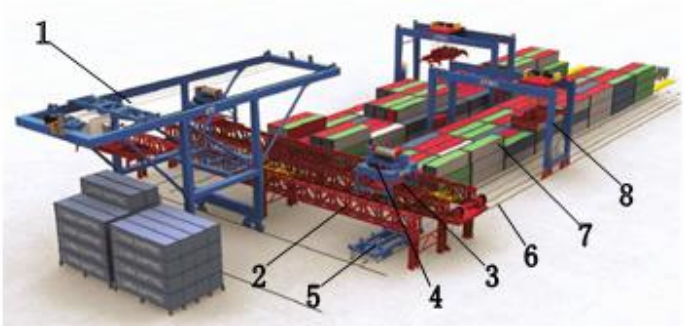

1. container crane; 2. low bridge; 3. container transport vehicle; 4. container lifting vehicle; 5. ground rotary container vehicle; 6. ground track; 7. yard; 8. track crane

Figure 1. Virtual Reality Simulation for Automated Container Terminal (ACT)

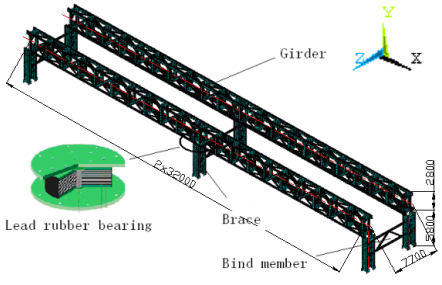

Figure 2. Structural Schematic Diagram of Low Bridge

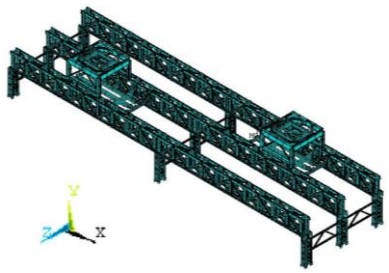

Figure 3. Vehicle-Bridge FEM Model

2.2. Container Vehicle-Low Bridge System Model

The container vehicle and the low truss bridge finite element method (FEM) model were established, as shown in Figure 3. The truss bridge and each vehicle are divided into free-interface subcomponents. Track model is not established and wheel degree of freedoms (DOFs) and rail DOFs are considered as the interface freedoms of vehicle and truss bridge respectively.

Assume that there is no relative displacement between rail and truss beam, considering self-excitation (track irregularity and lateral hunting movement), thus the bridge interface displacement

$$^{\mathrm{B}}\boldsymbol{u}_j = {}^{\mathrm{B}}\boldsymbol{u}_{\mathrm{v}j} + \boldsymbol{u}_{\mathrm{h}j} + \boldsymbol{u}_{\mathrm{s}j} \tag{1}$$

Where, $^{\mathrm{B}}\boldsymbol{u}_{\mathrm{v}j}$, $\boldsymbol{u}_{\mathrm{h}j}$, $\boldsymbol{u}_{\mathrm{s}j}$ are the bridge interface displacement, wheel set hunting movement and track irregularity vectors respectively[12].

Also assume that: (1) Wheel is a rigid body always contacted with rail, that is, the wheels do not jump; (2) Small displacement vibration of both vehicle and bridge; (3) Neglect effect from vehicle longitudinal movement on the bridge vibration and vehicle velocity. Interface compatible conditions are utilized to assembly VB coupled vibration system equation [6, 7].

LRB is a common device for seismic isolation and energy consumption, and widely used in bridges and constructions for its merits of simple structure, easy manufacture, and convenient installation and so on. Because of LRB's complicated non-linear characteristic, researchers usually adopt the equivalent linear model or the bilinear model in current analysis and design. According to the equivalent linear model, mechanical characteristic parameters of the LRB are listed in Table 1.

Table 1. Mechanical Characteristic Parameters of the LRB

Type	Mass *m* (kg)	Vertical Stiffness K_v (N/m)	Equivalent Horizontal Stiffness k_B (N/m)
GZY300	56	1.188×10^6	1.13×10^3
GZY400	126	1.85×10^6	1.69×10^3
GZY500	228	1.972×10^9	1.91×10^6

2.3. Numerical Simulation of Track Irregularity and Wind Load Stochastic Processes

By considering of weak correlation between different directions, the Shinozuka's method [13] was utilized to simulate one-variant multidimensional homogeneous process. Such left track (LT) and right track (RT) lateral and vertical irregularity is illustrated in Figure 4. Moreover, PSD of simulated sample is observed to agree with the target, one example is as shown in Figure 5.

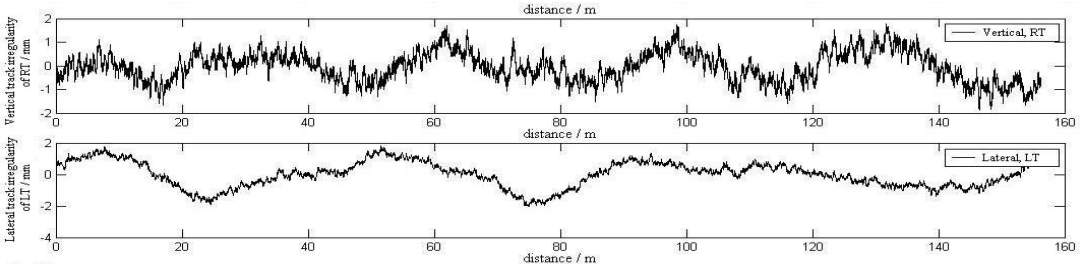

Figure 4. Vertical or Lateral Track Irregularity Curve of the Left or Right Track

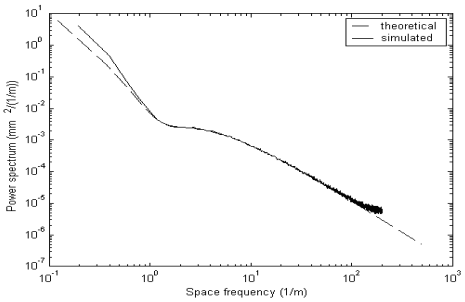

Figure 5. Comparison of the Theoretical Spectrum and the Simulated Spectrum of the Left Track's Vertical Irregularity

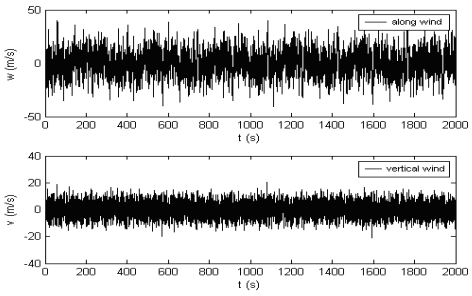

Figure 6. Time History of Along-Wind and Vertical-Wind Fluctuating Wind Velocity ($\bar{U}(10) = 60\text{m/s}$)

In this paper, Kaimal spectrum and Lumley-Panofsky spectrum were selected to simulate along-wind and vertical-wind, if $\bar{U}(10) = 60\text{m/s}$, along-wind and vertical-wind velocity time-history curves are illustrated in Figure 6.

2.4. Self-excitation Vibration Simulation and Model Test Results Comparison

Take Force, Length and Time as fundamental dimension system ([F,L,T]), structural dynamic similarity principles can be derived via dimensional analysis. Similarity principles and similarity constants for main physical variables can be obtained (refer to Appendix I). The designed model is shown in Figure 7.

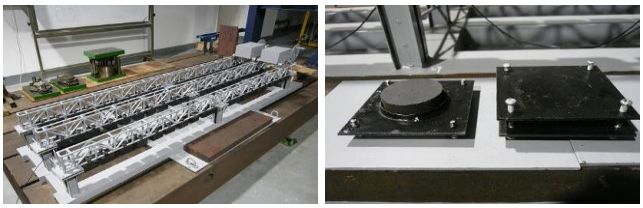

Figure 7. Photos of the Truss Bridge and the LRB Models

Under full rigid or flexible support constraint, self-excitation test maximum response and simulation values are listed in Table 2.

Table 2. Maximum Acceleration Response Comparison of Model Test and Prototype Simulation

Prototype Vehicle Speed (m/s)	Support Form	Maximum Acceleration Response of Bridge (m/s^2)				Maximum Acceleration Response of Vehicle (m/s^2)			
		Vertical		Lateral		Vertical		Lateral	
		Test	Simulation	Test	Simulation	Test	Simulation	Test	Simulation
4	rigid	2.05	1.54	0.15	0.16	0.26	0.069	0.32	0.220
	flexible	1.37	1.32	0.14	0.12	0.22	0.063	0.29	0.218
6	rigid	2.07	1.60	0.20	0.20	0.38	0.129	0.61	0.410
	flexible	1.70	1.34	0.16	0.15	0.41	0.126	0.48	0.397
8	rigid	2.23	1.65	0.19	0.24	0.49	0.223	0.81	0.634
	flexible	1.80	1.38	0.18	0.20	0.55	0.238	0.73	0.576

Table 2 presents that the model test acceleration response and simulation value agree with each other very well. The vehicle-bridge response value increases with vehicle velocity. Moreover, under full flexible support, the responses are obviously less than that under full rigid supports, which indicates that the LBR can effectively reduce the acceleration response.

When the vehicle speed is 4m/s and one line is on operation (single-running), lateral acceleration of the middle span of the bridge with full rigid supports and vehicle acceleration, lateral acceleration response prototype simulation and model test time-history curves of the truss bridge and the vehicle (v_V=4m/s) are shown in Figure 8 and Figure 9.

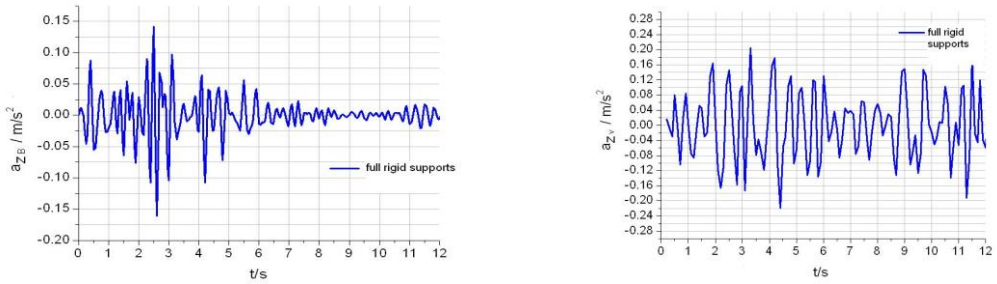

a) Lateral acceleration of the middle span b) Lateral acceleration of the vehicle

Figure 8. Lateral Acceleration Response Prototype Simulation Time-History Curves of the Truss Bridge and the Vehicle (v_V=4m/s)

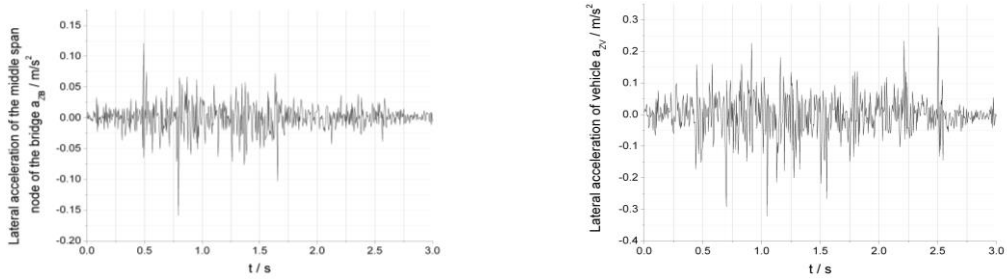

a) Lateral acceleration of the middle span b) Lateral acceleration of the vehicle

Figure 9. Lateral Acceleration Response Model Test Time-History Curves of the Bridge and Vehicle (v_V=4m/s)

By comparing Figure 8 to Figure 9, the vehicle-bridge vibration waveforms are the same as the simulation. Dynamic time-history analysis and model test verifies that the model design is reasonable and Dual-compatible CMS method is feasible to solve the coupled vibration of the VB system.

3. Structural Safety Assessment of the Container Vehicle-Low Bridge System

3.1. Vehicle-bridge Safety Evaluation Standard

(1) Bridge safety assessment standards

a. Deflection-span ratio threshold: for continuous truss bridges, vertical deflection caused by a moving train must be lower than L/900, L is the span. But lateral limit is not provided

(refer to TB10002.1-99). Japan's truss bridge specification takes the lateral value as half of the vertical deflection, that is, L/1800 [3]. For the truss bridge here, vertical and lateral deflections are 0.036m and 0.018m respectively.

b. Acceleration threshold: EUROCODE indicates the vertical acceleration maximum must be 0.5g and specifies the limit as 1.4m/s^2 (0.14g) [12].

(2) Vehicle running safety assessment standards

At present, running safety is quantified by the derailment coefficient, wheel load reduction rate and wheel transverse rocking force. This paper apply this out-rail geometric criteria to evaluation. It is defined by the wheel shift $|\mu_s|$ and transverse offset of wheel relative to the rail $|\Delta|$. When both conditions are satisfied the wheel will run out of the rail. In this case, $|\mu_s|$ and $|\Delta|$ can be determined as 25mm and 37.5mm by the wheel-rail contact relationship.

(3) Running stationarity assessment standards

This parameter can be evaluated by the indices of vehicle body acceleration. GB5599-85 suggests that vertical and lateral acceleration limit of the train body is lower than 0.7g and 0.5g respectively.

3.2. Structural Safety Assessment under Wind Load

When vehicles double-running, both vertical static deflection y_s and lateral static deflection z_s vary with the mean velocity $\bar{U}$ illustrated in Table 3. From Table 3, static vertical and lateral deflections and dynamic deflections comply with TB10002.1-99.

Table 3. Maximum Vertical and Lateral Static Deflection, Wheel-Rail Relative Displacement vs. Mean Velocity of the Fluctuating Wind (The Truss Bridge Rigid Supported)

$\bar{U}$ / m/s	20	25	30	35	40	45	50	55	60
y_s / mm	10.1	10.2	10.3	10.5	10.6	10.8	10.9	11.0	11.1
z_s / mm	4.14	4.53	5.02	5.59	6.25	7.00	7.84	8.77	9.78
$\|\mu_s\|$ / mm	10.3	10.8	11.6	12.1	12.7	13.2	13.9	15.0	15.5
$\|\Delta\|$ / mm	5.94	6.90	8.15	9.55	11.0	12.4	14.1	16.6	19.2

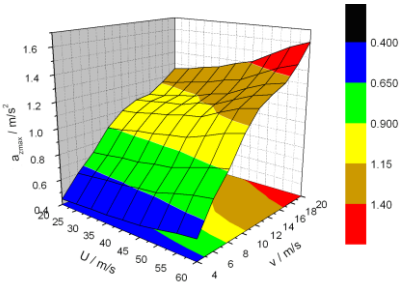

Figure 10. Maximum Lateral Acceleration Response of the Truss Bridge vs. v_V and $\bar{U}$

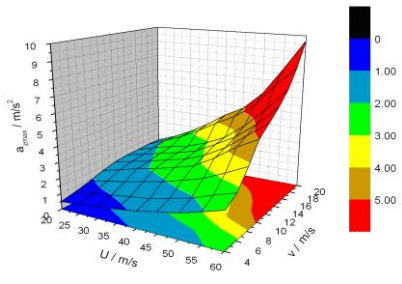

Figure 11. Maximum Lateral Acceleration Response of the Vehicle vs. v_V and $\bar{U}$

Figure 10 presents that lateral acceleration of the bridge increases with the vehicle speed and wind velocity. So does the vertical acceleration. When the vehicle speed and mean wind velocity are 20m/s and 60m/s respectively, vertical acceleration reaches 2.43m/s^2.

According to acceleration standard, vertical acceleration value is below 0.5g. However, when wind velocity is larger than 45m/s and the vehicle speed larger than 20m/s, or when wind velocity is larger than 55m/s and the vehicle speed larger than 18m/s, the lateral acceleration is beyond the limit, 0.14g by TB10002.1-99 standard.

Vertical and lateral relative displacement maximum can be referred in Table 3. .According to derailment geometric condition, $|\mu_s| \geq 25\text{mm}, |\Delta| \geq 37.5\text{ mm}$, when wind velocity is below 60m/s and vehicle speed below 20m/s, the vehicle is safe. It is noted that wheel-rail relative displacement errors do exist and thus stationarity indictor must be examined further.

From Figure 11, lateral acceleration rises with the two velocities. When the vehicle speed and mean wind velocity are 20m/s and 60m/s respectively, vertical acceleration reaches 9.68m/s^2. Vertical acceleration satisfies the similar trend and its maximum is 2.31m/s^2, far below the lateral value.

According to the vehicle running stationarity assessment standard, vertical acceleration maximum is out of reach of the threshold 0.7g by GB5599-85 standard. However, when wind velocity is larger than 50m/s and the vehicle speed larger than 18m/s, or when wind velocity is larger than 55m/s and the vehicle speed larger than 14m/s, the lateral acceleration is beyond the limit, 0.5g by TB10002.1-99 standard.

In summary: (1) Deflection-span ratio and acceleration indices are suggested to assess the bridge safety. That is, deflection-span is examined first, acceleration indices next. (2) Lateral acceleration of the vehicle and bridge probably go beyond the threshold, especially for the vehicle. (3) When the vehicle runs at the designed speed of 4m/s and mean wind velocity less than 60m/s, indicators are far less than the standard limit, which indicates the structural safety and running stationarity are good. And when on full rigid supports, the vehicle velocity can be raised to 8m/s.

When mean wind velocity is below 60m/s and the vehicle speed below 20m/s, the maximum coupled vibration response of vehicle-bridge on full rigid supported and full LRB supported are compared in Table 4.

Table 4. Comparison of the Maximum Vehicle-Bridge Coupled Vibration Response when the Truss Bridge Rigid Supported and LRB Supported

Coupled Vibration Results	Rigid	LRB	Standard limits
Vertical static and dynamic deflection / mm	11.1/32.7	13.3/35.3	36
Lateral static and dynamic deflection / mm	9.78/11.5	14.2/15.0	18
Vertical acceleration of bridge/ m/s^2	2.43	2.04	5
Lateral acceleration of bridge / m/s^2	1.61	1.35	1.4
Lateral acceleration of vehicle / m/s^2	9.68	4.64	5
Vertical relative displacement of wheel-rail / mm	15.5	22.8	25
Lateral relative displacement of wheel-rail / mm	19.2	21.2	37.5

From the table, consistent to the model test results, LRB can reduce acceleration obviously. For example, in the above case, the vehicle and bridge acceleration decrease down the limit. However, LRB will increase lateral deflection and wheel-rail relative displacement which can be controlled down the limit by certain LRB model. In a word, if full rigid supported theme is changed into full LRB supported theme, vehicle speed can be raised to 20m/s.

3.3. VB Coupled Vibration Response under Seismic and Operational Wind Load

One typical seismic code, such as EI Centro wave was applied to the vehicle-bridge system and neglected multi-point excitation and traveling-wave effect. In simulation, mean wind velocity and lateral seismic acceleration were taken 20m/s and 0.34g respectively, because that Typhoon (or storms, hurricanes) and earthquake this two kinds of extreme external environment excitation occur at the same time is very unlikely. The starting point is properly selected to assure the occurrence of maximum acceleration. On full rigid supports, when the vehicle is running at 4m/s in two line way, the vertical and lateral displacement and acceleration in the middle of the bridge with and without seismic load is compared in Figure 12 a), b), c).

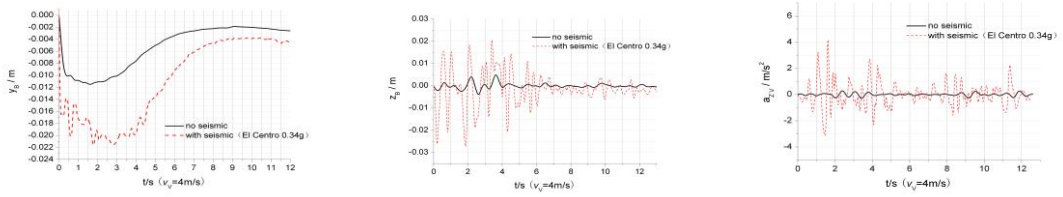

a) Vertical displacement b) Lateral displacement c) Lateral acceleration

Figure 12. The Dynamic Response Comparison of the Vehicle-Bridge Vibration Under either Seismic Load or Not

Figures 12 presents that when seismic load applied, the maximum response and frequency value become larger than that without earthquake load. For example, the displacement and acceleration in middle span under seismic load is 1.9, 4.6 and 12.4 times than that without. Furthermore, vertical displacement time-history in middle span presents moving vehicle load is significant for the coupled vibration and that seismic load mainly affects the amplitude. However, in lateral vibration analysis, all time-history curve is similar to EI Centro wave, which state that seismic load is main cause, compared to operational wind load and self-excitation. Therefore, if the construction site probably suffers from rarely occurred earthquake, seismic load must be considered in the design.

3.4. Structural Safety Assessment under Seismic and Operational Wind Load

Lateral acceleration maximum trend of the vehicle and the middle span of the truss bridge on two kinds of supports vs. seismic intensity and the vehicle speed are shown in Figure 13 and Figure 14.

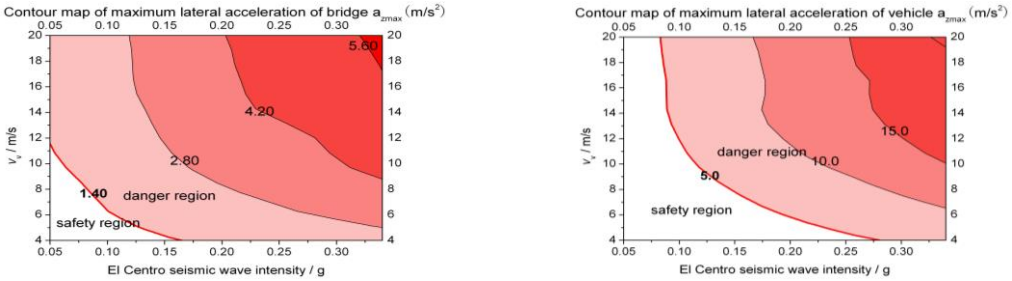

a) Max. lateral acceleration of bridge b) Max. lateral acceleration of vehicle

Figure 13. Ground Motion Intensity and Vehicle Speed Limits for Structural Safety when Rigid Supported

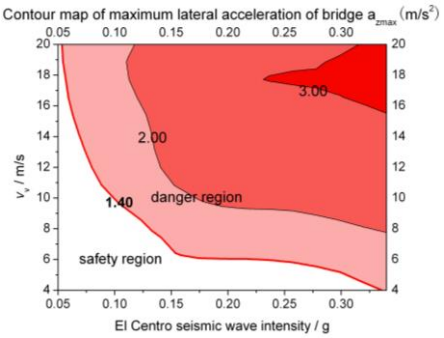

a) Max. lateral acceleration of bridge

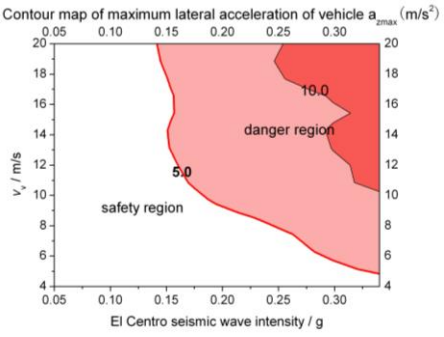

b) Max. lateral acceleration of vehicle

Figure 14. Ground Motion Intensity and Vehicle Speed Limits for Structural Safety when LRB Supported

By comparing Figure 13 and 14 to Figure 10 and 11, the sensitivity of the response to the seismic load is greater than the wind load. Illustrated in Figure 13, 14, safety zone of taking lateral acceleration of bridge as assessment indicator is smaller than that of the vehicle, which indicates that the bridge suffers more serious from seismic load. In contrast, Figure 10, 11 reflect the opposite regulation, which means the vehicle suffers more serious from wind load. That's because ground motion is from the ground upwards while containers on the vehicle have a large frontal area. Meantime, LRB can obviously enlarge the safety zone.

By the El Centro wave excitation, when the vehicle speed is 4m/s, seismic intensity threshold of the bridge on full rigid or flexible supports are 0.16g and 0.33g; when the vehicle speed reaches 6m/s, seismic intensity thresholds of the bridge change to 0.10g, 0.20g; when the vehicle speed ranges from 8 to 10 m/s, the thresholds reduce to 0.05g and 0.10g; at last, when the vehicle speed ranges from 10 to 20 m/s, the thresholds reduce to 0.05g and 0.05g again.

Due to the fact that the predominant period of El Centro wave is near to the first order natural frequency of the truss bridge, the seismic intensity and the vehicle speed limit under the El Centro excitation can be considered as the designed safety threshold. Furthermore, full flexible support is suggested as the truss bridge support type. In conclusion, a safety factor is taken into account, when the seismic intensity is below 0.3g, 0.2g, and 0.1g, 0.05g, the vehicle speed limit is suggested to be 4m/s, 6m/s, 8m/s, 20m/s respectively.

The above analyses were based on the conditions that the vehicles were running on the bridge during earthquake. Assume the vehicle stops in the position of middle span, still input El Centro wave and operational wind load, when LRB supported, the vertical and lateral deflection meets TB10002.2-2005 provisions. Therefore, ground vibration acceleration monitoring sensor can be set in the automated terminal, when the intensity limit reaches, the container vehicle decelerate to stop immediately to ensure the safety of the structure.

4. Conclusions

(1) The results of model test and prototype simulation prove with each other, which confirm the method of applying free-interface CMS to solve vehicle-bridge coupled vibration problem, also validates LRB's effects on vibration isolation as well as vehicle speed's influence on coupled vibration response.

(2) In the three-dimensional distribution container vehicle-low bridge system of automated container terminal, vertical coupled vibration of the container vehicle-truss bridge system is caused mainly by the vehicle moving load, and self-excitation is a major factor. Wind,

seismic load will greatly enhance the lateral vibration. As vehicle speed, fluctuating wind average velocity or ground motion intensity increases, the response increases. And the sensitivity of the response to the seismic load is greater than the wind load.

(3) On evaluating the truss bridge's safety, first evaluate by deflection-span ratio. Then, acceleration indices can be used to assess further. Moreover, the vehicle running stationarity shall be estimated by the lateral acceleration of the vehicle.

(4) The truss bridge is suggested to use LRB supported form. Thus, under wind load (wind velocity<60m/s) without seismic load, the vehicle can reach 20m/s. Moreover, under operational wind (wind velocity=60m/s) and ground motion (EI Centro wave) excitation simultaneously, when the seismic intensity is below 0.3g, 0.2g, 0.1g, 0.05g, the vehicle speed can reach up to 4m/s, 6m/s, 8m/s and 20m/s respectively. However, when the intensity is up to 0.3g, the vehicle must be stopped immediately.

Acknowledgements

This work is sponsored by Shanghai Top Academic Discipline Project- Management Science & Engineering, this paper is supported by Doctoral Fund of the Ministry of Education Jointly Funded Project (20123121120002) and Shanghai Education Committee Project "Shanghai Young College Teacher Training Subsidy Scheme", also supported in part by Ministry of Transport Research Projects (2012-329-810-180), Shanghai Municipal Education Commission Project (12ZZ148, 12ZZ149, 13YZ080).

References

[1] Y. L. Xu, Z. Nan and X. He, "Vibration of coupled train and cable-stayed bridge system in cross wind", Bridge Engineering, the American Society of Civil Engineers (ASCE), vol. 26, no. 1, **(2004)**, pp. 1389-1306.
[2] G. Weiwei, X. He and Y. L. Xu, "Dynamic response of long span suspension bridge and running safety of train under wind action", Engineering Mechanics, vol. 23, no. 2, **(2006)**, pp. 103-110.
[3] Z. Qingyuan and G. Xiangrong, "Vibration analysis of train-bridge time-varying system: theory and application", China Railway Press, Beijing, **(1999)**.
[4] L. Yongle, Q. Shizhong and L. Haili, "Study on wind velocity field for the coupling vibration of wind-vehicle-bridge system", Acta Aerodynamica Sinca, vol. 24, no. 1, **(2006)**, pp. 131-136.
[5] H. Yan, X. He and Z. Nan, "Dynamic response analysis of Train-Bridge system under non-uniform seismic excitations", China Railway Science, vol. 27, no. 5, **(2006)**, pp. 46-53.
[6] Y. B. Yang, "Vehicle-bridge interaction analysis by dynamic condensation method", Structural Engineering, the American Society of Civil Engineers (ASCE), vol. 121, no. 11, **(1995)**, pp. 1636-1643.
[7] L. Kailiang, Q. Huiqing and M. Fei, "Free-interface component mode synthesis technique with link substructure as super-element", Journal of Tongji University (Natural Science), vol. 38, no. 8, pp. **(2010)**, pp. 1215-1220,1233.
[8] X. He and Z. Nan, "Vehicle and structure dynamic interaction (2nd edition)", Science Press, Beijing, **(2005)**.
[9] M. Shinozuka and C. M. Jan, "Digital simulation of random process and its application", Journal of Sound and Vibration, vol. 25, no. 1, **(1972)**, pp. 111-128.
[10] H. A. Capers and M. M. Valeo, "FHWA's International Scan on Ensuring Bridge Safety and Serviceability", Transportation Research Record: Journal of the Transportation Research Board, vol. 2202, no. 4, **(2010)**, pp. 117-123.
[11] S. S. Law and J. Li, "Updating the reliability of a concrete bridge structure based on condition assessment with uncertainties", Engineering Structures, vol. 32, no. 1, **(2010)**, pp. 286-296.
[12] L. Wu, L. Zhang and J. Zhou, "The Safety Assessment Model of Stone Arch Bridge Based on Fuzzy Synthetic Evaluation", JDCTA: International Journal of Digital Content Technology and its Applications, vol. 6, no. 6, **(2012)**, pp. 43-52.
[13] C. Ming, "Fuzzy Integrated Evaluation Algorithm of Existing Bridge Based on Grid", AISS: Advances in Information Sciences and Service Sciences, vol. 3, no. 4, **(2011)**, pp. 141-146.

Appendix I

According to the Buckingham's π theorem, consider a physical phenomenon having *n* physical variables $x_1, x_2, x_3, \cdots, x_n$ and *k* basic dimensions (L, M, T or L, F, T or such) used to describe them. The phenomenon can be expressed by the relationship among $n–k=m$ non-dimensional groups $\pi_1, \pi_2, \pi_3, \cdots, \pi_m$. The equation expressing the phenomenon as a function *f* of the physical variables

$$f(x_1, x_2, \text{L L }, x_n) = 0 \tag{A-1}$$

Function (A-1) can be substituted by the following equation expressing it as a function F of a smaller number of non-dimensional groups:

$$F(p_1, p_2, \text{L L }, p_m) = 0 \tag{A-2}$$

In order to produce $\pi_1, \pi_2, \pi_3, \cdots, \pi_m$, *k* core physical variables are selected which do not form a π by themselves. Each π group will be a power product of these with each one of the *m* remaining variables. The powers of the physical variables in each π group are determined algebraically by the condition that the powers of each basic dimension must sum to zero.

If *m* π groups of the model equals these of the prototype $\pi_{im} = \pi_{ip}$, then both prototype and model are similar. The dimensional analysis will be performed to produce the dynamic-similarity laws below.

The parameters relevant to dynamic model test include stress σ, strain ε, elastic stiffness *E*, passion ratio μ, density ρ, length *l*, angular displacement θ, area *A*, tense load *F*, linear load *q*, mass *m*, stiffness *k*, damp *c*, natural period *T*, velocity *v*, acceleration *a*, gravity *g*, *etc*. Strain, Poisson's ratio and angular displacement are dimensionless quantities. Thus, $c_\varepsilon = c_\mu = c_\theta = 1$. Other parameters, such as volume, frequency, can be expressed by length l and time T in the dimensional analysis. Take force, length and time (F,L,T) as fundamental unit system, we can obtain unit matrix

	E	*r*	*l*	*s*	*A*	*F*	*q*	*p*	*M*	*γ*	*m*	*k*	*c*	*T*	*v*	*a*	*g*
F	1	1	0	1	0	1	1	1	1	1	1	1	1	0	0	0	0
L	-2	-4	1	-2	2	0	-1	-2	1	-3	1	-1	-1	0	1	1	1
T	0	2	0	0	0	0	0	0	0	0	2	0	1	1	-1	-2	-2

From this unit system, we can achieve three linear homogenous formulations of rank three. Take elastic modulus, density, length as basic quantities, we can obtain π matrix and π terms below.

p_n	E	r	l	s	A	F	q	p	M	γ	m	k	c	T	v	a	g
$p_1 = s/E$	-1	0	0	1	0	0	0	0	0	0	0	0	0	0	0	0	0
$p_2 = A/l^2$	0	0	-2	0	1	0	0	0	0	0	0	0	0	0	0	0	0
$p_3 = F/(El^2)$	-1	0	-2	0	0	1	0	0	0	0	0	0	0	0	0	0	0
$p_4 = q/(El)$	-1	0	-1	0	0	0	1	0	0	0	0	0	0	0	0	0	0
$p_5 = p/E$	-1	0	0	0	0	0	0	1	0	0	0	0	0	0	0	0	0
$p_6 = M/(El^3)$	-1	0	-3	0	0	0	0	0	1	0	0	0	0	0	0	0	0
$p_7 = g/(E/l)$	-1	0	1	0	0	0	0	0	0	1	0	0	0	0	0	0	0
$p_8 = m/(rl^3)$	0	-1	-3	0	0	0	0	0	0	0	1	0	0	0	0	0	0
$p_9 = k/(El)$	-1	0	-1	0	0	0	0	0	0	0	0	1	0	0	0	0	0
$p_{10} = \frac{c}{(Er)^{1/2}l^2} = \frac{c}{El^{3/2}}$	-1/2	-1/2	-2	0	0	0	0	0	0	0	0	0	1	0	0	0	0
$p_{11} = \frac{TE^{1/2}}{r^{1/2}l} = \frac{T}{l^{1/2}}$	1/2	-1/2	-1	0	0	0	0	0	0	0	0	0	0	1	0	0	0
$p_{12} = v/(E/r)^{1/2} = v/l^{1/2}$	-1/2	1/2	0	0	0	0	0	0	0	0	0	0	0	0	1	0	0
$p_{13} = a/(E/rl)$	-1	1	1	0	0	0	0	0	0	0	0	0	0	0	0	1	0
$p_{14} = g/(E/rl)$	-1	1	1	0	0	0	0	0	0	0	0	0	0	0	0	0	1

Take gravitational acceleration similarity ratio $c_g = 1$, and then $c_\rho = c_E / c_l$; dynamic-similarity conditions can be obtained (in Table I) by the above π terms.

Table I. Similarity Principles of Dynamic Structural Model Test

Physical Variables	Dimension	Similarity Principles	Similarity Constants
Length l	[L]	c_l	1/30
Mass m	$[FL^{-1}T^2]$	$c_m = c_r c_l^3$	$1/30^2$
Stiffness k	$[FL^{-1}]$	$c_k = c_E c_l$	1/30
Damp c	$[FL^{-1}T]$	$c_c = c_E c_l^{3/2}$	$1/30^{3/2}$
Density r	$[FL^{-4}T^2]$	$c_r = c_E / c_l$	30
Time(period)T	[T]	$c_t = c_l^{1/2}$	$1/\sqrt{30}$
Velocity v	$[LT^{-1}]$	$c_v = c_l^{1/2}$	$1/\sqrt{30}$
Acceleration a	$[LT^{-2}]$	$c_a = c_E / (c_r\ c_l)$	1

Author

LU Kai-liang, received his PhD from Tongji University, Shanghai, China. Currently, he is working in Logistics Engineering College, Shanghai Maritime University (SMU) as a lecturer. His research interests include port machine structure and system dynamics, theory and method of dynamic design and optimization of structure, *etc*. He has 12 publications to his credit both in international and national Journals. He is a committee member of Shanghai Society of Theoretical & Applied Mechanics, member of China Construction Machinery Society (CCMS), and Logistics Engineering Institution, CMES.